Journal of Orthopaedic Translation (2019) 19, 106—117

Available online at www.sciencedirect.com

ScienceDirect

journal homepage: http://ees.elsevier.com/jot

ORIGINAL ARTICLE

Sargassum integerrimum inhibits oestrogen deficiency and hyperlipidaemia-induced bone loss by upregulating nuclear factor (erythroid-derived 2)-like 2 in female rats

Kefeng Wu [a,1], Zhongqin Gong [b,1], Liyi Zou [c,1], Hua Ye [a], Changxiu Wang [d], Yangchun Liu [e], Yan Liang [f], Yanping Li [a], Jianwei Ren [g], Liao Cui [a,f,], Yi Liu [a,*]**

[a] *Guangdong Key Laboratory for Research and Development of Natural Drugs, Guangdong Medical University, Zhanjiang, Guangdong, 524023, China*
[b] *Shenzhen Ritzcon Biological Technology Co., Ltd., Shenzhen, 518000, China*
[c] *Department of Pharmacology, Guangdong Medical University, Dongguan, 523808, Guangdong, China*
[d] *School of Public Health, Guangdong Medical University, Dongguan, Guangdong, 523808, China*
[e] *Jiangxi Medical College, Queen Mary College of Nanchang University, Nanchang, Jiangxi, 330000, China*
[f] *Department of Pharmacology, Guangdong Medical University, Zhanjiang, Guangdong, 524023, China*
[g] *School of Biomedical Sciences, The Chinese University of Hong Kong, New Territories, Hong Kong, China*

Received 27 November 2018; received in revised form 17 February 2019; accepted 4 March 2019
Available online 27 March 2019

KEYWORDS
Bone loss;
Hyperlipidaemia;
Nrf2;
Oestrogen deficiency;
Oxidative stress;
Sargassum integerrimum

Abstract *Ethnopharmacological relevance:* Oestrogen deficiency, high incidences of hyperlipidaemia (HLP) and accelerated bone loss frequently occur in postmenopausal women. There is an urgent need to develop functional foods or specific drugs to protect against bone loss induced by oestrogen deficiency with HLP.
Aim of the study: In this study, we investigated the potential inhibitory effects of *Sargassum integerrimum* (SI) on bone loss in an ovariectomized rat model with HLP.
Materials and methods: The rats were treated for 12 weeks, and then, bone mineral density, bone biomechanical, bone microstructure, bone morphology, biomarkers of HLP oxidative

Abbreviations: OS, oxidative stress; HLP, hyperlipidaemia; SOD, superoxide dismutase; TOAC, total antioxidant capacity.

* Corresponding author. Guangdong Key Laboratory for Research and Development of Natural Drugs, Guangdong Medical University, Wenmingdong Road, Zhanjiang, 524023, Guangdong, China.
** Corresponding author. Guangdong Key Laboratory for Research and Development of Natural Drugs, Guangdong Medical University, Wenmingdong Road, Zhanjiang, 524023, Guangdong, China.
E-mail addresses: cuiliao@163.com (L. Cui), plliu78@sina.com (Y. Liu).
[1] These authors contributed equally to this work.

https://doi.org/10.1016/j.jot.2019.03.002

stress and side effects were determined. Immunohistochemical staining and Western blot were performed to evaluate related protein expression.
Results: The femur bone mineral density increased ($P < 0.05$), and the microscopic structures (ratio of bone volume to total volume [BV/TV], connectivity density [Conn.D], trabecular number [Tb.N] and trabecular thickness [Tb.Th]) of the bone trabecula and mechanical properties (maximum and breaking load [ML and BL, respectively]) improved after SI treatment ($P < 0.05$). Furthermore, the levels of HLP biomarkers (total cholesterol, triglyceride and low-density lipoprotein) were significantly decreased ($P < 0.05$), whereas the levels of antioxidant markers (superoxide dismutase and total antioxidant capacity) were increased ($P < 0.05$). Similar results were obtained with immunohistochemical staining, whereas the Western blot assay showed that SI stimulated the expression of nuclear factor (erythroid-derived 2)-like 2 (Nrf2) in bone.
Conclusion: Our data indicate that rats exposed to SI treatment for 12 weeks did not exhibit noticeable side effects. In conclusion, SI suppressed bone loss induced by ovariectomized and the associated HLP in rats by activating Nrf2, which could be a promising treatment option for osteoporosis induced by oestrogen deficiency and HLP in postmenopausal women.
Translational scope statement: Our study verified that SI prevented bone loss in rats with oestrogen deficiency with HLP by upregulating nuclear factor (erythroid-derived 2)-like 2. Furthermore, no side effect was observed after the long-term administration of SI. Those results suggested SI could be developed as a functional food or drug for postmenopausal osteoporosis induced by oestrogen deficiency with HLP.

Introduction

Postmenopausal osteoporosis (PMOP) is a chronic disease characterized by high fracture risk and low bone mass and strength, which has become a significant health hazard in postmenopausal women [1]. Oestrogen deficiency is considered the leading cause of PMOP [2], and unfortunately, accumulating evidence has shown that the hyperlipidaemia (HLP) incidence is higher in postmenopausal women than it is in premenopausal women [3]. Evidence also shows that HLP could accelerate bone loss in postmenopausal women, which exacerbates OP [4].

Currently, the most common therapy for PMOP is oestrogen replacement therapy (ERT), which not only effectively prevents bone loss induced by oestrogen deficiency [5] but also decreases serum lipid in postmenopausal women [6]. However, ERT has been found to increase the morbidity of some cancers, such as breast and endometrial cancers [7]. Interestingly, the 3-hydroxy-3-methylglutaryl coenzyme A reductase inhibitor statins, which have been used to decrease serum lipid, were reported to enhance new bone formation [8]. Nevertheless, statins cause some unusual side effects, which most prominently include myopathy, rhabdomyolysis and polyneuropathy [9]. Thus, there is an urgent need to develop effective and low toxicity functional foods or drugs for preventing bone loss induced by oestrogen deficiency with HLP.

Considerable research has shown that menopause and HLP induce oxidative stress (OS) [10,11]. OS involves biochemical disequilibrium and is caused by excessive production of free radicals and reactive oxygen species (ROS), which play a detrimental role in several human diseases such as cancer, atherosclerosis and OP. Oestrogen deficiency could induce OS, which acts as a possible trigger for PMOP [12], and evidence shows that OS is an early event in the development of HLP [13]. Therefore, antioxidants may play a crucial role in preventing bone loss induced by oestrogen deficiency with HLP.

Sargassum integerrimum (SI), a brown seaweed that specifically grows in Zhanjiang, China, has been used as a food item, and its antioxidant activity was recently demonstrated [14]. However, whether SI can prevent bone loss induced by ovariectomy and HLP is unclear. Therefore, in this study, we established a bilateral ovariectomized (OVX) rat model with HLP to examine the effects of SI on bone loss and explore its underlying mechanism. To the best of our knowledge, this is the first study to evaluate the effect of SI using an OP model.

Materials and methods

Preparation of SI

The SI, which belongs to the Phaeophyta phylum, was collected from the coast of Naozhou Island and identified by Enyi Xie, a professor at Guangdong Ocean University, in May 2014. After collection, the SI samples were placed on ice and immediately transported to the laboratory in insulated sealed ice boxes, to protect them from heat, air and light exposure. The fresh biomass was then cleaned with aqueous sodium chloride (NaCl) solution (3.5% m/m) to remove the epiphytes and encrusted material, freeze-dried and stored at −20 °C. The SI material was powdered,

extracted with water/ethanol (3:7, v/v to 10 volumes of the algal powder) for 24 h at room temperature with occasional agitation and then filtered. Subsequently, the extract was concentrated under reduced pressure, and the residue was freeze-dried to yield the crude SI powder, which was administered by gavage. A voucher specimen of this seaweed was preserved and deposited in the Guangdong Key Laboratory for Research and Development of Natural Drugs, Guangdong Medical University.

Animal treatments

Fifty-four 12-week-old, female Sprague—Dawley (SD) rats, weighing 200 ± 20 g, were acclimated to local vivarium conditions (temperature, 24—26 °C and humidity, 70%) and allowed free to access to diets and water. The experiment was conducted in accordance with special pathogen-free animal care approved protocols of the Animal Center of Guangdong Medical University, Zhanjiang, China. After adaptation, some rats were divided into the following groups (n = 9): sham operation (Sham, OVX and intraperitoneal poloxamer 407 (P407, BASF, Germany) injection (HLP) groups. The remaining rats, which underwent bilateral OVX and intraperitoneal P407 injections, were further divided into three groups (n = 9 each) as follows: OVX with HLP (OVX + HLP), OVX with HLP treated with SI (OVX + HLP + SI) and OVX with HLP treated with simvastatin (SVT) (Zhejiang Jingxin Pharmaceutical Co., Ltd., Zhejiang, China; OVX + HLP + SVT). After a 3-day postoperative recovery period, all rats were orally administered with deionized water. The HLP, OVX + HLP, OVX + HLP + SI and OVX + HLP + SVT groups were administered with intraperitoneal injections with P407 at a dose of 392 mg/kg body weight twice a week for 12 weeks. Furthermore, rats in the OVX + HLP + SI and OVX + HLP + SVT groups were treated with SI and SVT (350 and 14 mg/kg body weight, respectively) by gavage 5 times per week for 12 weeks (Table 1). All rats received subcutaneous injections with calcein (10 mg/kg, Sigma—Aldrich, St. Louis, MO, USA) on day 14, 13, 4 and 3 before euthanasia. All the rats were treated for 12 weeks postoperatively.

Table 1 Animal experimental design: treatment and dosage.

Groups	Description of treatment and dosage
Sham	Saline at a dose of 100 mL kg^{-1} d^{-1}
OVX	Saline at a dose of 100 mL kg^{-1} d^{-1}
HLP	P407 at a dose of 392 mg kg^{-1} d^{-1}
OVX + HLP	P407 at a dose of 392 mg kg^{-1} d^{-1} and saline at 100 mL kg^{-1} d^{-1}
OVX + HLP + SI	P407 at a dose of 392 mg kg^{-1} d^{-1} and SI at 350 mg kg^{-1} d^{-1}
OVX + HLP + SVT	P407 at a dose of 392 mg kg^{-1} d^{-1} and SVT at 14 mg kg^{-1} d^{-1}

Fifty-four SD rats were randomly divided into six groups. After a 3-day postoperative recovery period, sham-operated and OVX rats were administrated saline (1 mL/10 g body weight) via gavage, and the mice were maintained under standard conditions for 12 weeks. The HLP, OVX + HLP, OVX + HLP + SI, and OVX + HLP + SVT groups all received P407 intraperitoneal injections at 392 mg kg body weight-1·d-1 twice weekly. The OVX + HLP + SI and OVX + HLP + SVT groups were treated with SI (350 mg kg body weight-1·d-1 and SVT (14 mg kg body weight-1·d-1) for 5 days per week respectively.
SD, Sprague—Dawley; SI, Sargassum integerrimum; OVX, ovariectomized; HLP, hyperlipidaemia; SVT, simvastatin.

Sample collection and application

The rats were weighed weekly, and at the end point, they were euthanized by cardiac puncture under anaesthesia with sodium pentobarbitone. The serum was collected for biochemical assays, while the left femur was dissected for bone mineral density (BMD) determination, bone biomechanical property evaluation and measurement of trabecular micro—computed tomography (CT) analysis. The left proximal tibia metaphysis (PTM) was processed into undecalcified sections to observe the formation using appropriate labelling, whereas the right PTM was cut into decalcified sections for immunohistochemical (IHC) staining. The right femur was dissected for Western blot analysis.

Serum biomarker assay

The blood samples were collected in specimen tubes and kept at 25 °C for 40—50 min in a vertical position until clotting was complete. Then, the serum was separated by centrifuging at 1000×*g* for 10 min and stored at −80 °C for biochemical marker assays. The serum lipid (total cholesterol, triglyceride and low-density lipoprotein cholesterol [LDL]), serum antioxidant marker (total antioxidant capacity [TAOC], superoxide dismutase [SOD], glutathione peroxidase [GSH-PX] and methane dicarboxylic aldehyde [MDA]) and serum toxicity marker (blood urea nitrogen, creatinine, alanine aminotransferase and aspartate aminotransferase) levels were determined using colorimetric assays based on enzyme-driven reactions with commercial kits (Nanjing Jiancheng Biological Bioengineering, Nanjing, Jiangsu, China) using the ELX 800 microplate reader (Bio-tek Instruments, Winooski, VT, USA) as per the manufacturer's protocol.

BMD determination

The left femurs of the rats were moisturized by soaking in saline solution, and the residual muscle was removed and stored at −80 °C. The whole femur and lumbar BMD was measured with a dual energy X-ray absorptiometry (DXA) system, the Lunar Prodigy Advance Bone Densitometer (GE Healthcare Bio-Sciences Corp., Piscataway, NJ, USA) [15].

Evaluation of bone biomechanical properties

The left femurs were used to determine the bone mechanical properties through three-point bending using a material testing machine (H25KS; Hounsfield Test Equipment Ltd., UK). Before mechanical testing, the femurs were taken out from the freezer and thawed overnight. The femurs were positioned horizontally to the base with the anterior surface upward and centred on the supports

10 mm apart. The maximum load and the energy to failure (energy resorption) were calculated using built-in software (QMAT Professional; Tinius Olsen Inc. Horsham, PA, USA) [16].

Micro-CT analysis

The fourth lumbar vertebrae were scanned using a desktop preclinical specimen micro-CT (μCT-40; Scanco Medical, Bassersdorf, Switzerland). Briefly, the vertebral bodies were aligned perpendicular to the scanning axis for a total scanning length of 6.0 mm at a custom isotropic resolution of 8-μm isometric voxel size with a voltage of 70 kV p and a current of 114 lA. Three-dimensional (3D) reconstructions of mineralized tissues were performed by an application of a global threshold (211 mg hydroxyapatite/cm^3), and a Gaussian filter (sigma = 0.8, support = 2) was used to suppress noise. A volume of interest containing only trabecular bone within the vertebral body extracted from the cortical bone with 1.80-mm thick (150 slices) was acquired 1.0—1.2 mm from both cranial and caudal growth plate—metaphyseal junctions. The 3D reconstructed images were used directly to quantify microarchitecture, and the morphometric parameters including bone volume fraction (BV/TV), trabecular number (Tb.N, 1/mm), trabecular thickness (Tb.Th, mm), trabecular separation (Tb.Sp, mm) and connective density (Conn.D, 1/mm^3) were calculated with the image analysis program of the microCT workstation (Image Processing Language, v4.29d; Scanco Medical, Switzerland) [17].

Bone histomorphometry

The bone histomorphometry experimental protocol used was based on that of a previous study [18]. Briefly, the right proximal tibial metaphyses were embedded undecalcified in methyl methacrylate, and then 8-μm-thick frontal sections were cut using an RM2155 hard tissue microtome (Leica, Wetzlar, Germany). Then, a digitizing image analysis system (Osteometrics, Inc., Decatur, GA, USA) was used for the quantitative bone histomorphometry measurements.

IHC staining

The right PTM was fixed in 4% paraformaldehyde for 12 h at room temperature, decalcified with ethylenediaminetetraacetic acid decalcifying solution for 4 weeks and then finally stored in 70% ethanol. The PTM was permeated with xylene and embedded in paraffin, and the frontal PTM tissues were cut into 4-μm-thick sections using the RM2155 hard tissue microtome. Then, the sections were mounted on glass slides coated with egg white—glycerol or polylysine, dried for 1 h at 60 °C and stored at 4 °C for IHC staining. Commercially available antibodies were incubated with the sections to detect bone morphogenetic protein 2 (BMP2), peroxisome proliferator-activated receptor-γ (PPARγ), and ROS. The ROS antibody was from Biosynthesis Biotechnology (Bioss, Beijing, China), and those for other target proteins were from Boster Biotechnology (Boster, Wuhan). The paraffin sections were deparaffinized, rehydrated and then incubated in deionized water containing 0.3% hydrogen peroxide—methanol for 30 min at room temperature to block endogenous peroxide. After washing with distilled water, the sections for ROS and BMP2 detection were exposed to trypsin, while those for PPARγ were placed in a microwave oven for antigen retrieval and then blocked with 5% bovine serum albumin. The sections were incubated with primary antibodies at the recommended dilution at 4 °C overnight and then with the secondary antibody for 30 min at 37 °C. Then, the sections were incubated with streptomycin avidin reagent, finally counterstained with Mayer's haematoxylin to identify the nuclei and then mounted with Permount. Photomicrograph images were captured using a Nikon Eclipse E400 camera (Nikon, Japan) with the Picture Frame software. The images were analysed using the ImagePro Plus 6.0 software (Media Cybernetics), and the average optical density (AOD) of the positive area of each specimen was obtained.

Western blot analysis

The right femur of each rat was ground using liquid nitrogen, the total protein was extracted using the Western blotting and immunoprecipitation cell lysis kit (Beyotime, Jiangsu, China) and then it was stored at −80 °C until used. The Western blot analysis was performed as follows: an equal volume of 6 × sodium dodecyl sulphate sample buffer was added to the protein samples, which were boiled for 5 min, separated using electrophoresis on 10% sodium dodecyl sulphate—polyacrylamide gels for 45 min at 80V, followed by 100 min at 100 V, and then were transferred onto a polyvinylidene difluoride membrane. The membrane was blocked with 5% skimmed milk for 2 h under room conditions and then hybridized for 1 h with nuclear factor (erythroid-derived 2)-like 2 (Nrf2; Abcom, HK) at 1:500, and β-actin (1:1000; Santa Cruz Biotechnology, Santa Cruz, CA, USA) was used as a loading control. The membrane was washed six times with phosphate-buffered saline (plus Tween 20 for 10 min each time, incubated with horseradish peroxidase—conjugated secondary antibody for 2 h and then visualized using ECL Plus Western Blot Detection Reagents (GE Healthcare Life Sciences, Tokyo). The protein bands were digitized using an Epson perfection 2480 scanner (Seiko Corp, Nagano, Japan), and the Nrf2 expression levels were normalized to β-actin.

Statistical analysis

The data were presented as means ± standard deviation (SD) and analysed using the statistical package for the social sciences (SPSS) 16.0 software for Windows (SPSS, Chicago, IL, USA). The statistical differences among groups were analysed using an analysis of variance and Tukey's honestly significant difference post hoc test. A P-value < 0.05 was considered significant.

Results

SI inhibits bone loss induced by oestrogen deficiency with HLP in female rats

First, to assess whether SI inhibits bone loss induced by OVX with HLP in female rats, we examined the BMD of the left femur and the fifth lumbar vertebrae (LV5). The BMD of the femurs of the OVX + HLP group was significantly decreased than that of the Sham group ($P < 0.01$), whereas that of the LV5 was not significantly different between the Sham and OVX + HLP groups. These results indicate that oestrogen deficiency with HLP decreased the BMD of female rats. Interestingly, after SI treatment for 12 weeks, the BMD values of the femur and LV5 were both increased compared with those of the OVX + HLP group ($P < 0.01$ and $P > 0.05$, respectively, Figure 1A and B).

Second, we examined the biomechanical properties of the femur bone, and as shown in Figure 1 C, D, E & F, no significant differences were observed between the OVX + HLP and Sham groups. However, the elastic load, breaking load, bone rigidity coefficient and maximum load of the OVX + HLP group were lower than those of

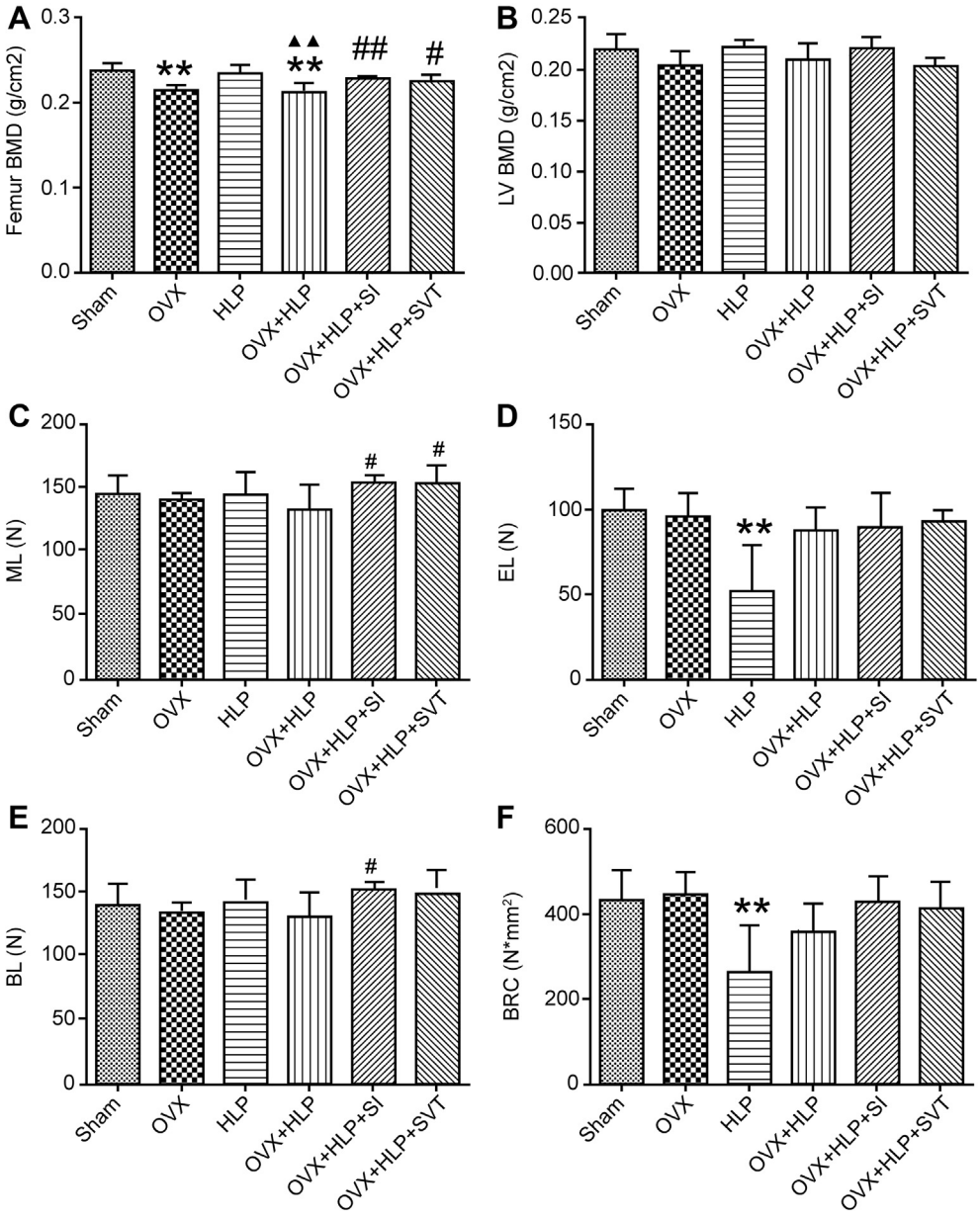

Figure 1 SI improves BMD and biomechanical properties of bone in oestrogen deficiency with HLP mice. (A) and (B) the BMD of left femur and LV5, respectively. (C), (D), (E) and (F) The femur biomechanical properties (EL [N], BL [N], ML [N], BRC [N*mm^2]). Values are means ± SD. *$P < 0.05$ and **$P < 0.01$ vs. Sham; ●$P < 0.05$ and ●●$P < 0.01$ vs. OVX; ▲$P < 0.05$ and ▲▲$P < 0.01$ vs. HLP; and $^{\#}P < 0.05$ and $^{\#\#}P < 0.01$ vs. OVX + HLP. SD, standard deviation; BMD, bone mineral density; HLP, hyperlipidaemia; OVX, ovariectomized; SVT, simvastatin; EL, elastic load; BL, breaking load; BRC, bone rigidity coefficient; ML, maximum load; SI, *Sargassum integerrimum*.

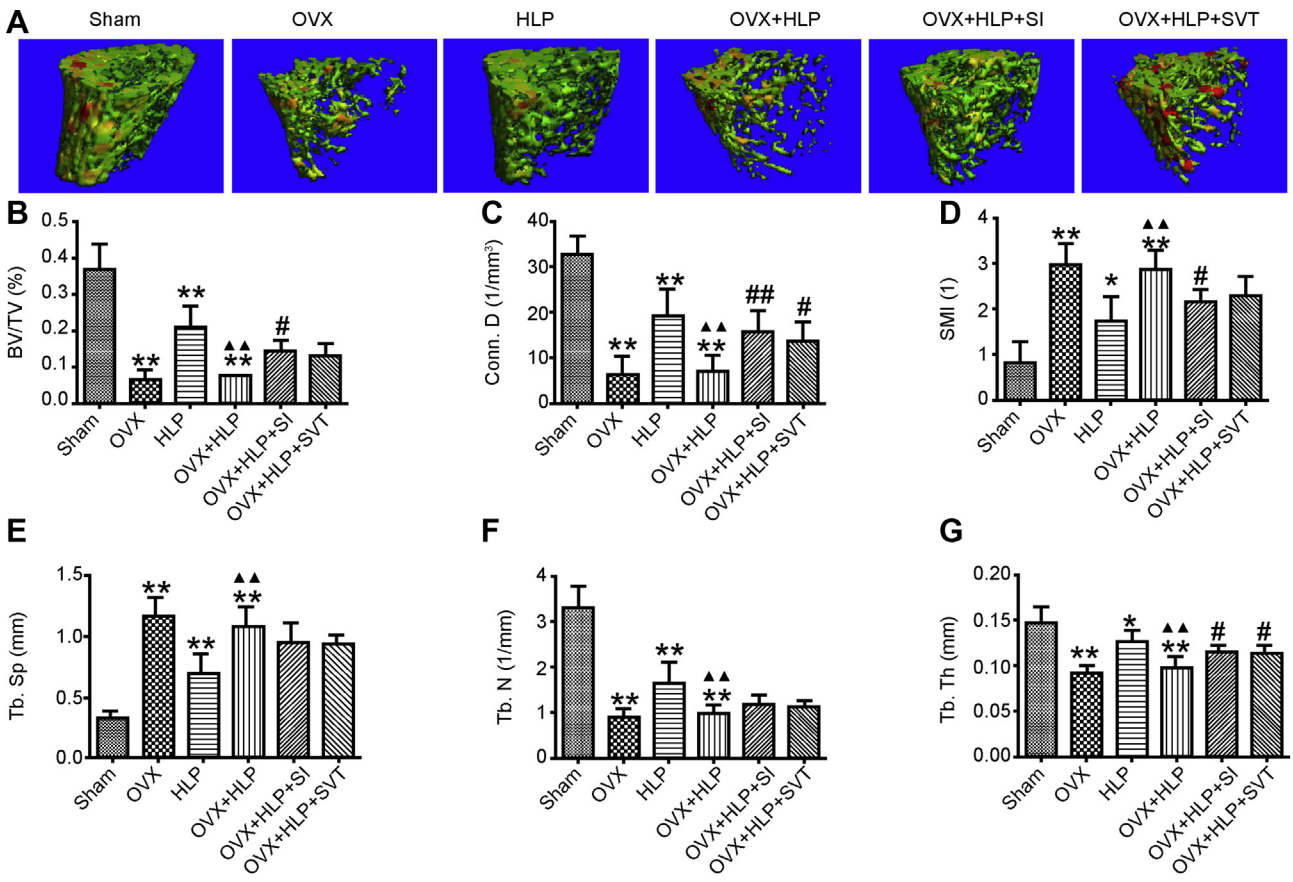

Figure 2 SI improves microarchitecture of the bone in oestrogen deficiency with HLP mice. The 3D reconstruction of trabecular representative images and trabecular microarchitecture (BV/TV, Conn.D, SMI, Tb.Sp, Tb. N and Tb. Th) of the left femur. Values are means ± SD. *P < 0.05 and **P < 0.01 vs. Sham; ●P < 0.05 and ●●P < 0.01 vs. OVX; ▲P < 0.05 and ▲▲P < 0.01 vs. HLP; and #P < 0.05 and ##P < 0.01 vs. OVX + HLP. HLP, hyperlipidaemia; OVX, ovariectomized; SD, standard deviation; SI, *Sargassum integerrimum*; 3D, three-dimensional.

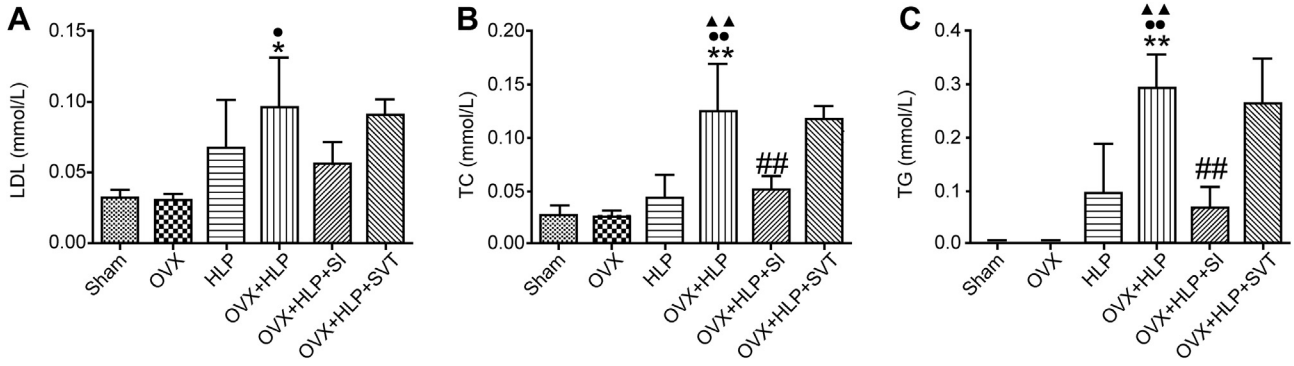

Figure 3 SI decreased serum lipid level. Serum lipid level markers were evaluated using commercial kits. (A) Serum TC level, (B) concentration of LDL and (C) serum TG level. Values are means ± SD. *P < 0.05 and **P < 0.01 vs. Sham; ●P < 0.05 and ●●P < 0.01 vs. OVX; ▲P < 0.05 and ▲▲P < 0.01 vs. HLP; and #P < 0.05 and ##P < 0.01 vs. OVX + HLP. TC, total cholesterol; TG, triglyceride; LDL, low-density lipoprotein; HLP, hyperlipidaemia; OVX, ovariectomized; SD, standard deviation; SI, *Sargassum integerrimum*.

the Sham group. In the SI group, the maximum load and breaking load were significantly increased (P < 0.05 vs. the OVX + HLP group) and the bone rigidity coefficient and elastic load values were increased with no significant differences compared with the OVX + HLP group.

Third, we used micro-CT to examine the trabecular microarchitecture of the femurs. The representative 3D reconstructed images are shown in Figure 2A. The trabecular microarchitecture (ratio of bone to total volume [BV/TV], connectivity density [Conn.D], trabecular number [Tb.N], trabecular thickness [Tb.Th]) of the OVX rats with

Table 2 The quantitative result of fluorescence labelling (sL. Pm, dL. Pm, IrL. Wi).

Groups	sL. Pm (mm)	dL. Pm (mm)	IrL. Wi (μm)	MAR (μm/d)	BFR/BV (%/year)
Sham	13.2 ± 1.8	11.5 ± 1.6	13.6 ± 0.8	1.36 ± 0.08	25.83 ± 2.08
OVX	10.9 ± 2.3	14.2 ± 1.5	20.5 ± 4.5*	2.05 ± 0.45*	41.26 ± 4.25
HLP	12.7 ± 2.6	6.9 ± 1.9*	7.3 ± 5.6*	0.73 ± 0.56*	19.85 ± 1.78
OVX + HLP	1.4 ± 2.0*	0.9 ± 2.3**	5.8 ± 2.7	0.58 ± 0.26	2.11 ± 0.07
OVX + HLP + SI	9.7 ± 1.7##	10.9 ± 2.2##	10.6 ± 1.6#	1.06 ± 0.16#	25.86 ± 2.55
OVX + HLP + SVT	8.0 ± 1.9##	7.7 ± 3.3##	9.6 ± 3.1	0.96 ± 0.31#	20.38 ± 3.11

Values are means ± SD. *P < 0.05 and **P < 0.01 vs. Sham; P < 0.05 and P < 0.01 vs. OVX; P < 0.05 and P < 0.01 vs. HLP; and #P < 0.05 and ##P < 0.01 vs. OVX + HLP.
sL.Pm, single label perimeter; dL.Pm, double label perimeter; Ir.L.Wi, interlabel width; MAR, mineralization deposition rate; BFR, bone formation rate; BV, bone volume; OVX, ovariectomized; HLP, hyperlipidaemia; SD, standard deviation; SI, Sargassum integerrimum; SVT, simvastatin.

HLP was significantly disrupted compared with that of the Sham rats (P < 0.05). The BV/TV, Tb.Th (both P < 0.05) and Conn.D (P < 0.01) were significantly increased after SI treatment, whereas the structure model index was decreased (P < 0.05) compared with that of the OVX + HLP group (Figure 2B–G). These results suggest that SI improved the microarchitecture of the bone of OVX rats with HLP.

Finally, we examined the effect of SI on bone formation (Suppl. Figure 1), and Table 2 shows that the single label perimeter (sL. Pm), double label perimeter (dL. Pm), interlabel width (IrL. Wi), mineralization deposition rate (MAR) and bone formation rate (BFR) of the OVX + HLP group were decreased (P < 0.05) and no apparent fluorescent labelling was observed in the OVX rats with HLP,

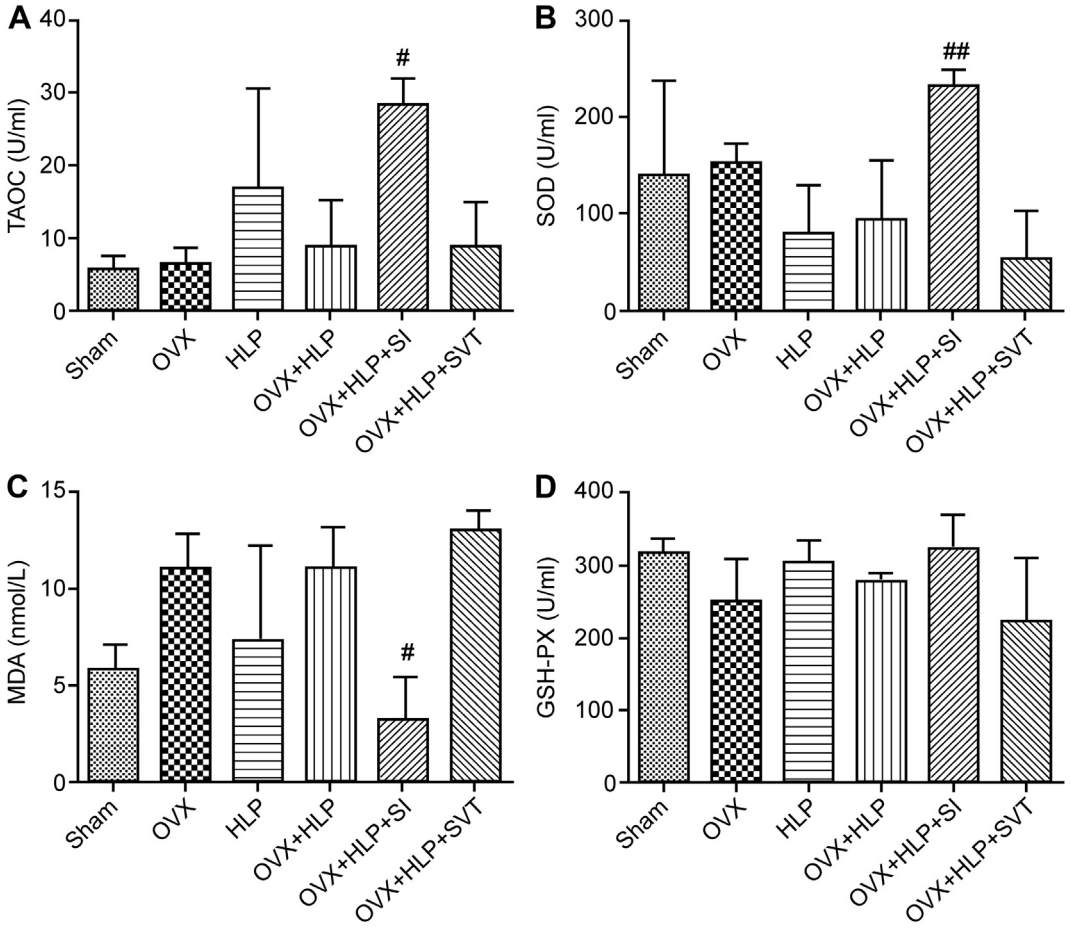

Figure 4 SI decreased oxidative stress in OVX rats with HLP. All biomarkers of OS: (A) TAOC, (B) SOD, (C) MDA and (D) GSH-PX were tested using kits. Values are means ± SD. #P < 0.05 and ##P < 0.01 vs. OVX + HLP. HLP, hyperlipidaemia; OVX, ovariectomized; SD, standard deviation; SI, *Sargassum integerrimum*; OS, oxidative stress; TAOC, total antioxidant capacity; SOD, superoxide dismutase; GSH-PX, glutathione peroxidase; MDA, methane dicarboxylic aldehyde.

indicating that OVX with HLP significantly inhibited bone formation. After treatment with SI, these parameters (sL. Pm, dL. Pm, IrL. Wi, MAR and BFR/BV) were significantly increased ($P < 0.05$) compared with those of the OVX + HLP group. SI and SVT both increased the bone formation and bone mass compared with those of the OVX + HLP group.

These results suggest that HLP accelerated bone loss in OVX-induced oestrogen deficient female rats, whereas SI reversed this severe effect.

SI decreases serum lipid level in OVX rats with HLP

To evaluate whether the anti−bone loss effect of SI is associated with antihyperlipidemia, we examined some serum HLP biomarkers. As shown in Figure 3, SI treatment decreased the concentrations of the triglyceride and total cholesterol ($P < 0.01$, vs. the VOX + HLP group) and the LDL level declined slightly. These results indicate that SI not only prevented bone loss but it also improved HLP.

SI decreases OS by increasing Nrf2 expression in OVX rats with HLP

To explore the underlying mechanism of the anti−bone loss effects of SI, biomarkers of OS were examined. As shown in Figure 4, the serum levels of GSH-PX, TAOC and SOD were downregulated, whereas that of MDA was upregulated in the OVX + HLP group, suggesting that OVX with P407 injection induced OS in rats. However, SI reduced OS by increasing the GSH-PX, TAOC and SOD (all $P < 0.05$) levels and decreasing MDA level ($P < 0.05$) in OVX rats with HLP.

To evaluate the expression of the bone formation, OS and adipogenesis markers (BMP2, ROS and PPARγ, respectively) in the tibia, we performed IHC staining and analysed the positively stained areas. The AOD of BMP2−positively stained area in the OVX, HLP and OVX + HLP groups was lower ($P < 0.01$, Figure 5) than that in the Sham group. SI and SVT significantly increased BMP2 expression in OVX rats with HLP. The AOD of the ROS− and PPARγ−positively

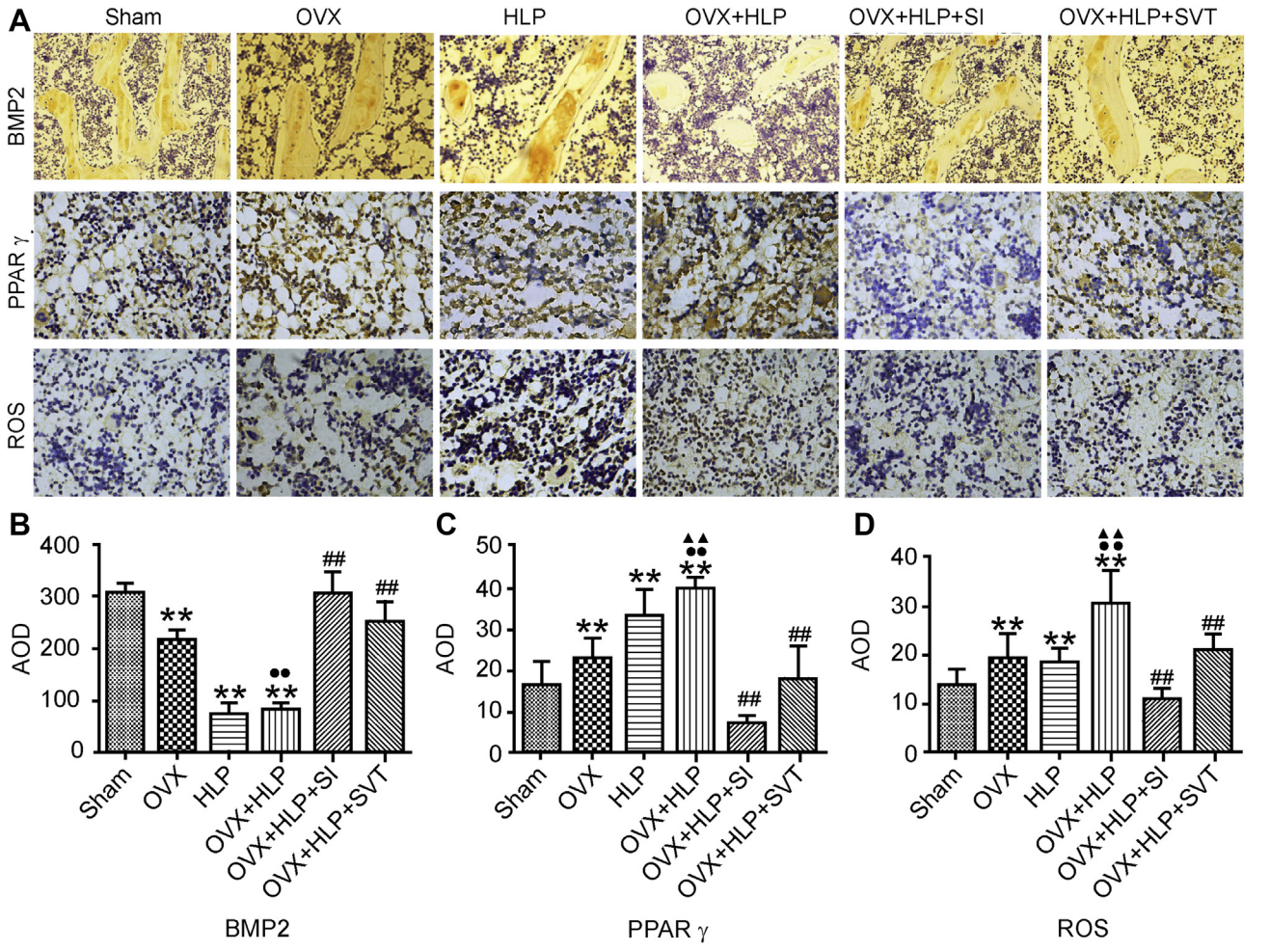

Figure 5 SI decreases the expression of ROS. The expression levels of BMP2, PPARγ and ROS were detected using IHC staining. Values are means ± SD. *$P < 0.05$ and **$P < 0.01$ vs. Sham; ●$P < 0.05$ and ●●$P < 0.01$ vs. OVX; ▲$P < 0.05$ and ▲▲$P < 0.01$ vs. HLP; and #$P < 0.05$ and ##$P < 0.01$ vs. OVX + HLP. HLP, hyperlipidaemia; OVX, ovariectomized; SD, standard deviation; SI, *Sargassum integerrimum*; ROS, reactive oxygen species; BMP2, bone morphogenetic protein 2; PPARγ, peroxisome proliferator-activated receptor-γ; IHC, immunohistochemical.

stained areas in the OVX, HLP and OVX + HLP rats was higher ($P < 0.01$, Figure 5) than that in the Sham rats. However, the expression levels of ROS and PPARγ were significantly decreased after SI and SVT treatment ($P < 0.01$, Figure 5).

The results of the Western blot analysis (Figure 6) revealed that the expression of Nrf2 was decreased in the OVX, HLP and OVX + HLP groups. However, the expression of Nrf2 was significantly increased after SI treatment ($P < 0.01$ vs. the OVX, HLP and OVX + HLP groups). The data suggest that SI reduced OS in female rats by upregulating Nrf2 expression.

Safety of long-term SI administration

In this study, we treated female rats with SI for 12 weeks, and then examined the potential side effects. As shown in Supplementary Figure 2, there was no difference between the SI-treated and Sham groups in body weight and concentrations of aspartate aminotransferase, alanine aminotransferase, blood urea nitrogen and creatinine. This result indicates that SI is safe for long-term use.

Discussion

We successfully established the OP with HLP rat model and used it to demonstrate the positive effects and underlying mechanism of SI. Bone is a dynamic organ that constantly undergoes bone resorption and formation mediated by osteoclasts and osteoblasts, respectively [19]. Oestrogen plays a critical role in bone metabolism balance. Furthermore, the increased morbidity of HLP in postmenopausal women compared with those who are premenopausal has been identified [20]. In addition, HLP-induced accelerated bone loss in postmenopausal women has been reported previously [4].

Presently, no specific drug has been developed for the therapy of HLP with OP in postmenopausal women. Therefore, it would be extremely expedient to develop a functional food or drug that protects against bone loss in postmenopausal women. First, the HLP with OP rat model should be established before further research studies are conducted. A typical method for establishing the OP animal model is bilateral OVX [21], and intraperitoneal injection of P407 has been widely used in establishing HLP models [22]. In this study, after bilateral OVX and P407 injections, high concentrations of serum lipids, low femur BMD and deteriorated bone biomechanical properties and microarchitecture were observed in the OVX rats. Therefore, this animal model could be used to evaluate the antibone loss effect of functional foods and new drugs. Brown seaweed has been reported to possess numerous biological activities [23] including anti-inflammation, antimicrobial, antihyperlipidemia and antioxidative. Recent research indicates that brown seaweed promotes osteoblastic differentiation [24,25]. Therefore, we hypothesized that the brown seaweed SI,

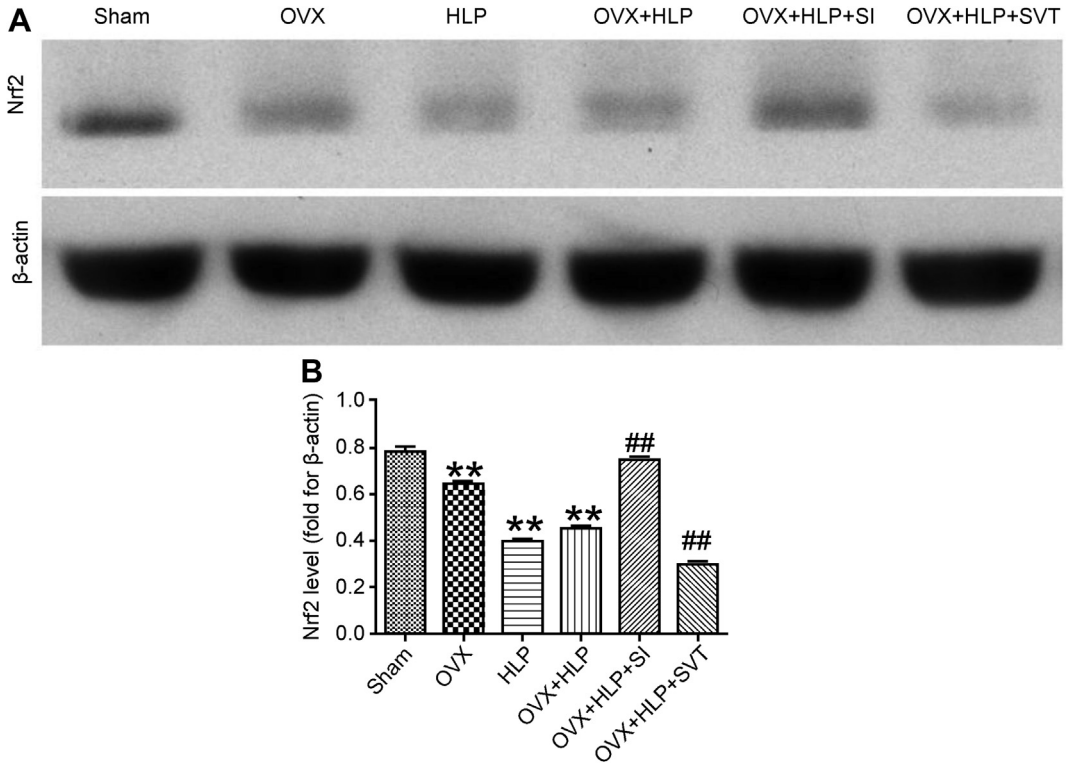

Figure 6 SI activates the level of Nrf2. Western blotting results and quantitative analysis of Nrf2 protein expression in different groups. β-Actin was the loading control. OVX, HLP and OVX + HLP significantly decreased protein expression of Nrf2, which reversed by SI. Values are means ± SD. *$P < 0.05$ and **$P < 0.01$ vs. Sham; $^{\bullet}P < 0.05$ and $^{\bullet\bullet}P < 0.01$ vs. OVX; $^{\blacktriangle}P < 0.05$ and $^{\blacktriangle\blacktriangle}P < 0.01$ vs. HLP; and $^{\#}P < 0.05$ and $^{\#\#}P < 0.01$ vs. OVX + HLP. HLP, hyperlipidaemia; OVX, ovariectomized; SD, standard deviation; SI, *Sargassum integerrimum*; Nrf2, nuclear factor (erythroid-derived 2)-like 2.

which specifically grows in Zhanjiang, might suppress bone loss induced by oestrogen deficiency with HLP. Our results illustrate that SI significantly increased the femur BMD and improved the bone biomechanical properties and bone microarchitecture.

OS plays a critical role in oestrogen deficiency—induced PMOP, while HLP also induces OS. The MDA concentration was higher, and GSH-PX value was lower in postmenopausal women than in women who are fertile [26]. A similar study also found that OVX induced OS in the femur bone of rats [27]. On the other hand, lower SOD activity was found in patients with HLP, and ROS production was positively correlated with either very low-density lipoprotein (VLDL) or LDL triglycerides [10]. Many studies indicate that OS can adversely affect bone homoeostasis, upregulate the activity of osteoclasts, enhance mesenchymal stem cells (MSCs) adipogenesis and inhibit osteogenic differentiation of mesenchymal stem cells, leading to extensive bone loss and fragility and aggravated morbidity and mortality of OP [28,29]. There has been a negative correlation between BMD and OS in human [30]. OS inhibits osteoblastic differentiation to bone cells through extracellular signal—regulated kinase and nuclear factor-κB signalling [31,32]. Moreover, OS antagonizes Wnt signalling in osteoblasts precursors by diverting β-catenin from T cell factor to forkhead box O—mediated transcription, resulting in lower new bone formation [33]. Some natural drugs have shown effects on anti-osteoporosis by decreasing OS [34]. The level of serum antioxidative markers (GSH-PX, SOD and TAOC) were increased by SI in OVX + HLP rats, suggesting that the effect of SI on bone loss induced by oestrogen deficiency with HLP is associated with decreased OS. The results of the IHC staining also confirmed these results. OVX with HLP increased ROS levels in the bone, but SI ameliorated this effect. The overexpression of PPARγ plays a crucial role in adipogenesis, which suggests a low bone mass in rodent [35]. In this study, we found that SI reduced the expression of PPARγ in the tibia. In contrast, the BMP2 expression was increased in the SI treatment group. BMP2, a member of the transforming growth factor beta superfamily of growth and differentiation factors, could mediate bone formation [24].

Nrf2 is one of the primary cellular defences against heightened oxidative stress, which is a master transcription factor that regulates induction of antioxidant gene expression and phase 2 antioxidant enzymes [36]. Studies also reported that Nrf2 counteracts oxidative stress and enhances adipogenesis by increasing the expression of PPARγ [37]. Extensive studies suggested that Nrf2 plays a crucial role in OP therapy. *In vitro*, some drugs protect osteoblastic cells against glucocorticoid damaged by increasing the expression of Nrf2 [38,39]. In addition, loss of Nrf2 accelerates ionizing radiation—induced bone loss by upregulating receptor activator of nuclear factor kappa-B ligand in rodents [40]. Furthermore, Nrf2 deficiency increases bone turnover, and its main effect is on bone resorption, and Nrf2 maintained bone microarchitecture *in vivo* [41]. Thus, a higher expression of Nrf2 is beneficial to the bone. The Western blot analysis result showed that SI significantly increased the expression of Nrf2.

In conclusion, SI prevented bone loss in rats with oestrogen deficiency with HLP. The underlying mechanism might be related to its antioxidative activity mediated by increasing the expression of Nrf2. No side effect was observed after the long-term administration of SI, which could be developed as a functional food or drug for PMOP induced by oestrogen deficiency with HLP.

Conflict of interest

The authors have no conflicts of interest to disclose in relation to this article.

Contributions of the authors

Wu Kefeng (winokhere@sina.com), Gong Zhongqin (gongzq01@163.com) and Zou Liyi (442516867@qq.com) prepared the SI, performed the animal experiments, analysed the data, participated in the study design and wrote the manuscript. Ye Hua (yehua2008@foxmail.com), Wang Changxiu (18343500@qq.com) and Liu Yangchun (Liuyangchun001@126.com) contributed to animal model establishment. Liang Yan (liangyan1008@qq.com) and Li Yanping (1293115317@qq.com) contributed to the micro-CT analysis. Yanping Li contributed to the IHC staining and Western blot analysis. Cui Liao (cuiliao@163.com) and Liu Yi (plliu78@sina.com) conceived the study design and participated in its development and coordination and helped in revising the manuscript. All authors contributed to the data analysis, drafting and revising the article and agree to be accountable for all aspects of the work. All authors read and approved the final manuscript for publication.

Funding

This work was supported by Science and Technology Project of Guangdong Province, China (grant number: 2017A040405052), Special Funds for Economic Development of Marine Economy of Guangdong Province, China (grant number: GDME-2018C011), Science and Technology Special Project of Zhanjiang, Guangdong, China (grant number: 2016A03014) and the Ph.D. Start-up Fund of Natural Science Foundation of Guangdong Medical University, Guangdong, China [grant number: B2017017]. The sponsors had no role in study design; collection, analysis and interpretation of data; writing of the report and decision to submit the article for publication.

Data statement

All data are available within the manuscript and its supplementary file.

Appendix A. Supplementary data

Supplementary data to this article can be found online at https://doi.org/10.1016/j.jot.2019.03.002.

References

[1] Kanis JA, Burlet N, Cooper C, Delmas PD, Reginster JY, Borgstrom F, et al. European guidance for the diagnosis and management of osteoporosis in postmenopausal women. Osteoporos Int 2008;19:399—428.

[2] Riggs BL, Khosla S, Melton 3rd LJ. A unitary model for involutional osteoporosis: estrogen deficiency causes both type I and type ii osteoporosis in postmenopausal women and contributes to bone loss in aging men. J Bone Miner Res 1998;13:763—73.

[3] Rosato V, Bosetti C, Talamini R, Levi F, Montella M, Giacosa A, et al. Metabolic syndrome and the risk of breast cancer in postmenopausal women. Ann Oncol 2011;22:2687—92.

[4] Tarakida A, Iino K, Abe K, Taniguchi R, Higuchi T, Mizunuma H, et al. Hypercholesterolemia accelerates bone loss in postmenopausal women. Climacteric 2011;14:105—11.

[5] Roberts JG, Webber CW, Woolever CA. Estrogen replacement therapy for postmenopausal osteoporosis. Can Fam Physician 1986;32:885—91.

[6] Crook D, Cust MP, Gangar KF, Worthington M, Hillard TC, Stevenson JC, et al. Comparison of transdermal and oral estrogen-progestin replacement therapy: effects on serum lipids and lipoproteins. Am J Obstet Gynecol 1992;166:950—5.

[7] Rossouw JE, Anderson GL, Prentice RL, LaCroix AZ, Kooperberg C, Stefanick ML. Risks and benefits of estrogen plus progestin in healthy postmenopausal women. J Am Med Assoc 2002;288:321—33.

[8] Edwards CJ, Hart DJ, Spector TD. Oral statins and increased bone-mineral density in postmenopausal women. Lancet 2000; 355:2218—9.

[9] Moosmann B, Behl C. Selenoprotein synthesis and side-effects of statins. Lancet 2004;363:892—4.

[10] Araujo FB, Barbosa DS, Hsin CY, Maranhão RC, Abdalla DS. Evaluation of oxidative stress in patients with hyperlipidemia. Atherosclerosis 1995;117:61—71.

[11] Mendoza CA, Zamarripa J. Menopause induces oxidative stress in Oxidative stress and chronic degenerative diseases-A role for antioxidants. In: Morales-González JA, editor. IntechOpen; 2013. p. 289—316.

[12] Sharma T, Islam N, Ahmad J, Akhtar N, Beg M. Correlation between bone mineral density and oxidative stress in postmenopausal women. Indian J Endocrinol Metab 2015;19: 491—7.

[13] Yang Y, Su Y, Wang D, Chen Y, Wu T, Li G, et al. Tanshinol attenuates the deleterious effects of oxidative stress on osteoblastic differentiation via wnt/foxo3a signaling. Oxidative Med Cel Longev 2013;2013:351895.

[14] Jin W, Zhang W, Wang J, Yao J, Xie E, Liu D, et al. A study of neuroprotective and antioxidant activities of heteropolysaccharides from six Sargassum species. Int J Biol Macromol 2014;67:336—42.

[15] Liu Y, Cui Y, Chen Y, Gao X, Su Y, Cui L. Effects of dexamethasone, celecoxib, and methotrexate on the histology and metabolism of bone tissue in healthy Sprague Dawley rats. Clin Interv Aging 2015;10:1245—53.

[16] Liu YY, Yao WM, Wu T, Xu BL, Chen F, Cui L. Captopril improves osteopenia in ovariectomized rats and promotes bone formation in osteoblasts. J Bone Miner Metab 2011;29: 149—58.

[17] Lin S, Huang J, Fu Z, Liang Y, Wu H, Xu L, et al. The effects of atorvastatin on the prevention of osteoporosis and dyslipidemia in the high-fat-fed ovariectomized rats. Calcif Tissue Int 2015;96:541—51.

[18] Cui L, Li T, Liu Y, Zhou L, Li P, Xu B, et al. Salvianolic acid B prevents bone loss in prednisone-treated rats through stimulation of osteogenesis and bone marrow angiogenesis. PLoS One 2012;7:2—17.

[19] Christenson RH. Biochemical markers of bone metabolism: an overview. Clin Biochem 1997;30:573—93.

[20] Arthur FK, Adu-Frimpong M, Osei-Yeboah J, Mensah FO, Owusu L. The prevalence of metabolic syndrome and its predominant components among pre-and postmenopausal Ghanaian women. BMC Res Notes 2013;6:446—57.

[21] Lelovas PP, Xanthos TT, Thoma SE, Lyritis GE, Dontas IA. The laboratory rat as an animal model for osteoporosis research. Comp Med 2008;58:424—30.

[22] Palmer WK, Emeson EE, Johnston TP. The poloxamer 407-induced hyperlipidemic atherogenic animal model. Med Sci Sports Exerc 1997;29:1416—21.

[23] Mhadhebia L, Mhadhebi A, Robert J, Bouraoui A. Antioxidant, anti-inflammatory and antiproliferative effects of aqueous extracts of three Mediterranean brown seaweeds of the genus. Cystoseira. Iran J Pharm Res 2014;13:207—20.

[24] Kim BS, Kang HJ, Park JY, Lee J. Fucoidan promotes osteoblast differentiation via JNK- and ERK-dependent BMP2-Smad 1/5/8 signaling in human mesenchymal stem cells. Exp Mol Med 2015;47:e128.

[25] So MJ, Cho EJ. Phloroglucinol attenuates free radical-induced oxidative stress. Prev Nutr Food Sci 2014;19:1293—5.

[26] Signorelli SS, Neri S, Sciacchitano S, Pino LD, Costa MP, Marchese G, et al. Behaviour of some indicators of oxidative stress in postmenopausal and fertile women. Maturitas 2006; 53:77—82.

[27] Muthusami S, Ramachandran I, Muthusamy B, Vasudevan G, Prabhu V, Subramaniam V, et al. Ovariectomy induces oxidative stress and impairs bone antioxidant system in adult rats. Clin Chim Acta 2005;360:81—6.

[28] Abdollahi M, Larijani B, Rahimi R, Salari P. Role of oxidative stress in osteoporosis. Therapy 2005;2:787—96.

[29] Tormos KV, Anso E, Hamanaka RB, Eisenbart J, Joseph J, Kalyanaraman B, et al. Mitochondrial complex III ROS regulate adipocyte differentiation. Cell Metabol 2011;14:537—44.

[30] Basu S, Michaëlsson K, Olofsson H, Johansson S, Melhus H. Association between oxidative stress and bone mineral density. Biochem Biophys Res Commun 2001;288:275—9.

[31] Bai XC, Lu D, Bai J, Zheng H, Ke ZY, Li XM, et al. Oxidative stress inhibits osteoblastic differentiation of bone cells by ERK and NF-κB. Biochem Biophys Res Commun 2004;314:197—207.

[32] Mody N, Parhami F, Sarafian TA, Demer LL. Oxidative stress modulates osteoblastic differentiation of vascular and bone cells. Free Radic Biol Med 2001;31:509—19.

[33] Hoogeboom D, Essers MA, Polderman PE, Voets E, Smits LM, Burgering BM. Interaction of FOXO with beta-catenin inhibits beta-catenin/T cell factor activity. J Biol Chem 2008;283:9224—30.

[34] Yang RL, Shi YH, Hao G, Li W, Le GW. Increasing oxidative stress with progressive hyperlipidemiain human: relation between malondialdehyde and atherogenic index. J Clin Biochem Nutr 2008;43:154—8.

[35] Ackert-Bicknell CL, Demissie S, Marin de Evsikova C, Hsu YH, DeMambro VE, Karasik D, et al. PPARG by dietary fat interaction influences bone mass in mice and humans. J Bone Miner Res 2008;23:1398—408.

[36] Jyrkkanen HK, Kansanen E, Inkala M, Kivelä AM, Hurttila H, Heinonen SE, et al. Nrf2 regulates antioxidant gene expression evoked by oxidized phospholipids in endothelial cells and murine arteries in vivo. Circ Res 2008;103:e1—9.

[37] Pi J, Leung L, Xue P, Wang W, Hou Y, Liu D, et al. Deficiency in the nuclear factor E2-related factor-2 transcription factor results in impaired adipogenesis and protects against diet-induced obesity. J Biol Chem 2010;285(12):9292—300.

[38] Lin H, Wei B, Li G, Zheng J, Sun J, Chu J, et al. Sulforaphane reverses glucocorticoid-induced apoptosis in osteoblastic cells through regulation of the Nrf2 pathway. Drug Des Dev Ther 2014;8:973—82.

[39] Lin H, Gao X, Chen G, Sun J, Chu J, Jing K, et al. Indole-3-carbinol as inhibitors of glucocorticoid-induced apoptosis in osteoblastic cells through blocking ROS-mediated Nrf2 pathway. Biochem Biophys Res Commun 2015;460:422—7.
[40] Ibanez L, Ferrandiz ML, Brines R, Guede D, Cuadrado A, Alcaraz MJ. Effects of Nrf2 deficiency on bone microarchitecture in an experimental model of osteoporosis. Oxid Med Cell Longev 2014;2014:726590.
[41] Rana T, Schultz MA, Freeman ML, Biswas S. Loss of Nrf2 accelerates ionizing radiation-induced bone loss by upregulating RANKL. Free Radic Biol Med 2012;53:2298—307.